Cooperative Effects in π-Ligand Bridged Dinuclear Complexes, Part XXI[≠]

Synfacially Structured [$(CpRu)_2\mu$-cot]—What a Difference the Coordination Side Makes!

Jürgen Heck,*[a] Gerhard Lange,[a] Maik Malessa,[a] Roland Boese,[b] and Dieter Bläser[b]

Dedicated to Professor Ernst Otto Fischer on the occasion of his 80th birthday

Abstract: By reaction of the neutral mononuclear complex [CpRu(1,2,3-η:6,7-η-C_8H_9)] (**1**) with [$(C_5R_5)Ru(MeCN)_3$]PF_6 (R = H, Me) the synfacial cationic μ-cyclooctatetraene-μ-hydrido-diruthenium complexes [(CpRu){(C_5R_5)Ru}(μ-H)(μ-cot)]PF_6 (cot = cyclooctatetraene; R = H: **2a**; R = Me: **2b**) are formed. Deprotonation of **2a** and **2b** with lithium diisopropylamide yields the synfacial homodinuclear complexes [(CpRu){(C_5R_5)Ru}μ-cot] (R = H: **3a**; R = Me: **3b**). Cyclic voltammetry studies of **3a** and **3b** show two clearly separated, electrochemically reversible one-electron redox waves 0/+1 and +1/+2 (0/+1: $E_{1/2}$(**3a**) = −0.79 V; $E_{1/2}$(**3b**) = −0.89 V; +1/+2: $E_{1/2}$(**3a**) = −0.17 V; $E_{1/2}$(**3b**) = −0.27 V versus [$FeCp_2$]/[$FeCp_2$]$^+$). Chemical oxidation of **3a** with [$FeCp_2$]$^+$ affords the monocation [**3a**]$^+$ and the dication [**3a**]$^{2+}$, depending on the stoichiometry. X-ray structure determination was performed on all dinuclear complexes. The complex **2a** and the neutral complex **3a** crystallize in the space groups *Cmcm* and $P\bar{1}$, respectively, and the monocationic species [**3a**]PF_6 in the space group *C2/c*. The dication [**3a**]$^{2+}$ crystallizes as the mixed salt [**3a**]$(BF_4)(PF_6)$ in the space group *Pnma*. In all the dinuclear complexes, the two metal centers are synfacially coordinated at the cot ligand. Complexes **2a** and **3a** show a η^4:η^4 bonding mode of the cot moiety, whereas, upon oxidation, the cot ligand in **3a** changes its hapticity to η^5:η^5. Results from ^{1}H NMR spectroscopic studies of **2a**, **2b** and [**3a**]$^{2+}$ are in accordance with the crystallographic findings, in contrast to the neutral complex **3a**, which shows a fast rotation of the cot entity even at 200 K. The Ru−Ru distances in the dinuclear complexes decrease dramatically from 307.8 pm in **2a** to 266 pm in [**3a**]$^{2+}$; complexes **3a** and [**3a**]$^+$ have Ru−Ru bond lengths of 295.6 and 282.2 pm, respectively. The Ru−Ru interaction in **2a** and **2b** can best be described as a three-center, two-electron RuHRu bond, whereas in **3a** and [**3a**]$^{2+}$ a Ru−Ru single bond must be considered. For the paramagnetic complex cation [**3a**]$^+$, a Ru−Ru σ* semi-occupied molecular orbital is postulated based on EPR and UV/Vis spectroscopic results, which indicate that [**3a**]$^+$ is a mixed-valent class III compound.

Keywords: coordination modes · cyclooctatetraene · metal–metal interactions · mixed-valent compounds · ruthenium

Introduction

Coordination chemists very rarely have the opportunity to monitor spectroscopic as well as geometrical changes of metal–metal bound dinuclear complexes in four successive differently charged states.[1] Our studies on metal–metal interactions in dinuclear μ-cot complexes[2, 3] presented us with such a stroke of luck when we attempted to synthesize the *synfacial* 34-valence electron (ve) complex [$(CpRu)_2\mu$-cot] (cot = cyclooctatetraene, Cp = cyclopentadienyl). The well known *antifacial* isomer of [$(CpRu)_2\mu$-cot][4a] shows some remarkable features. One is its diamagnetism, although each metal center formally bears 17 ve; a direct metal–metal bond can be excluded from the long Ru−Ru distance of 385.9 pm.[4b] Another remarkable feature is the two-electron oxidation at ambient temperature, which results in C−C bond cleavage of the cot ligand. As a consequence, a flyover dication is formed which enables a Ru−Ru single bond. Upon electrochemical reduction, only the antifacial complex [$(CpRu)_2\mu$-cot] is recovered (Scheme 1).[4b]

A major goal of the present work was to investigate the redox chemistry of a synfacially structured [$(CpRu)_2\mu$-cot] complex, which was suggested to be a stable isomer due to the

[a] Prof. Dr. J. Heck, Dr. G. Lange, Dipl.-Chem. M. Malessa
Institut für Anorganische und Angewandte Chemie der Universität
Martin-Luther-King-Platz 6, D-20146 Hamburg (Germany)
Fax: (+49) 40-4123-6348
E-mail: heck@chemie.uni-hamburg.de

[b] Prof. Dr. R. Boese, Dipl.-Chem. D. Bläser
Institut für Anorganische Chemie der Universität
Universitätsstrasse 5–7, D-45141 Essen (Germany)

[≠] Part XX: G. Bögels, H. C. Brussaard, U. Hagenau, J. Heck, J. Kopf, J. G. M. van der Linden, A. Roelofsen, *Chem. Eur. J.* **1997**, *3*, 1151–1159.

  0947-6539/99/0502-0659 $ 17.50+.50/0

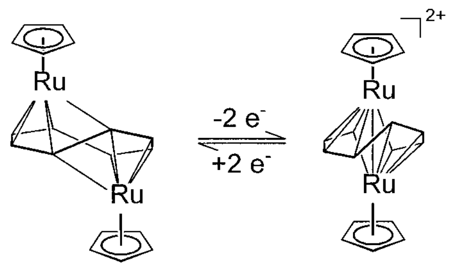

Scheme 1. Structures of the antifacial complexes [$(CpRu)_2\mu$-cot] and [$(CpRu)_2\mu$-$C_8H_8]^{2+}$.

34 ve. Is the stereochemistry (syn- or antifacial) decisive for the redox properties of [$(CpRu)_2\mu$-cot]? Earlier studies on synfacially coordinated dinuclear μ-cot complexes have shown only one-electron transfer reactions upon oxidation or reduction.[2, 3] As already known from antifacial [$(CpRu)_2\mu$-cot], the reaction pathway from an antifacial to a synfacial coordination mode by redox chemistry is impassable;[4b] does this also hold true for the opposite direction starting with a synfacial complex and ending up with the antifacial isomer?

Attempts were also made to synthesize synfacial [$(CpRu)_2\mu$-cot] derivatives by a stepwise alkyne tetramerization at a diruthenium center.[5] The linkage of four alkyne units was indeed successful, but the formation of a cyclooctatetraene complex failed; thermally induced ring closure reactions of an open chain C_8 unit to a cot ligand in dinuclear complexes were only successful for a dichromium complex.[6] In addition to this area of research, which is of substantial importance for the oligomerization of hydrocarbons at metal centers, we hoped that a better understanding of the metal–metal interaction and the coordination mode of the cot ligand would emerge.

Abstract in German: *Durch die Reaktion des neutralen einkernigen Komplexes [CpRu(1,2,3-η:6,7-η-C_8H_9)] (**1**) mit [$(C_5R_5)Ru(MeCN)_3]PF_6$ (R = H, Me) werden die synfacialen μ-Cyclooctatetraen-μ-hydrido-Komplexe [(CpRu){(C_5R_5)-Ru}(μ-H)(μ-cot)]PF_6 (R = H: **2a**; R = Me: **2b**) (cot = Cyclooctatetraen) gebildet; ihre Deprotonierung mit Lithiumdiisopropylamid führt zu den synfacialen homodinuklearen Komplexen [(CpRu){(C_5R_5)Ru}μ-cot] (R = H: **3a**; R = Me: **3b**). Cyclovoltammetrische Untersuchungen an **3a** und **3b** zeigen zwei deutlich getrennte, elektrochemisch reversible Redoxwellen, die den Einelektronenübergängen 0/+1 und +1/+2 zuzuordnen sind (0/+1: $E_{1/2}$(**3a**) = −0.79 V; $E_{1/2}$(**3b**) = −0.89 V; +1/+2: $E_{1/2}$(**3a**) = −0.17 V; $E_{1/2}$(**3b**) = −0.27 V vs. $[FeCp_2]/[FeCp_2]^+$). Eine chemische Oxidation von **3a** mit $[FeCp_2]^+$ ist möglich, die je nach Stöchiometrie der Reaktanden **3a** zum Monokation [**3a**]$^+$ oder zum Dikation [**3a**]$^{2+}$ oxidiert. Einkristallstrukturanalysen können an allen Zweikernkomplexen durchgeführt werden: **2a** und der Neutralkomplex **3a** kristallisieren in den Raumgruppen Cmcm beziehungsweise $P\bar{1}$, und das Monokation [**3a**]$^+$ als PF_6-Salz in der Raumgruppe C2/c; [**3a**]$^{2+}$ kristallisiert als Mischsalz [**3a**]$(BF_4)(PF_6)$ in der Raumgruppe Pnma. In allen zweikernigen Komplexen sind die Metallzentren synfacial am cot-Liganden koordiniert. **2a** und **3a** weisen einen η^4:η^4-Bindungsmodus der cot-Einheit auf, während nach der Oxidation von **3a** zum Mono- und Dikation der cot-Ligand seine Haptizität zur η^5:η^5-Form ändert.*
*Mit den kristallographischen Erkenntnissen stimmen die ^{1}H-NMR-spektroskopischen Ergebnisse von **2a**, **2b** und **3a**$^{2+}$ überein; dagegen zeigen sie für **3a** eine schnelle Rotation der cot-Einheit sogar noch bei 200 K. Die Ru-Ru-Abstände in den zweikernigen Komplexen nehmen von 307.8 pm in **2a** zu 266 pm in **3a**$^{2+}$ dramatisch ab; **3a** und [**3a**]$^+$ weisen eine Ru-Ru-Bindungslänge von 295.6 und 282.2 pm auf. Die Ru-Ru-Wechselwirkung in **2a** und **2b** kann am besten als 3c2e-Bindung beschrieben werden, wohingegen in **3a** und [**3a**]$^{2+}$ eine Ru-Ru-Einfachbindung angenommen werden muß. Für das paramagnetische Komplexkation [**3a**]$^+$ wird eine einfache Besetzung des Ru-Ru-σ*-Orbitals postuliert, im Einklang mit EPR- und UV-vis spektroskopischen Ergebnissen, die [**3a**]$^+$ als gemischt valenten Komplex der Klasse III ausweisen.*

Results and Discussion

Syntheses and spectroscopic features: Recently we reported that the synthesis of homo- and heterodinuclear μ-cot complexes results exclusively in synfacially configurated species when mononuclear cot[2] or cyclooctatrienyl[3] complexes with one non-coordinated carbon–carbon double bond within the *cyclo*-C_8 ligand were used as precursors. One example of this kind of mononuclear complexes is [CpRu(1,2,3-η:6,7-η-C_8H_9)] (**1**), which can be obtained from nucleophilic addition of a hydride ion to the cation [CpRu(η^6-cot)]$^+$ [7a] (Scheme 2).

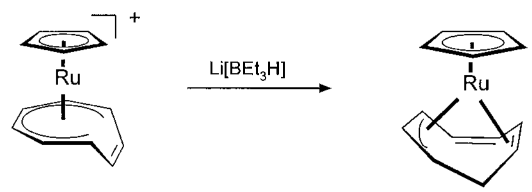

1

Scheme 2. Nucleophilic addition of a hydride to the coordinated cot ligand.

Complex **1**[8] was allowed to react with the half-sandwich compound [$(C_5R_5)Ru(MeCN)_3]PF_6$ (R = H, Me)[7a,b] to form the cationic hydrido complex [(CpRu){(C_5R_5)Ru}(H)(μ-cot)]PF_6 (R = H: **2a**; R = Me: **2b**) (Scheme 3). The cationic complexes **2a** and **2b** are easily deprotonated by lithium diisopropylamide (LDA) to form the neutral species [(CpRu){(C_5R_5)Ru}μ-cot] (R = H: **3a**; R = Me: **3b**). The ease of the deprotonation reaction is quite remarkable since earlier attempts failed to deprotonate dinuclear (μ-C_nH_n) hydrido complexes.[9]

Complexes **3a** and **3b** form orange-colored crystals and are sensitive to oxygen in solution. The redox potentials of **3a** and **3b**, determined by cyclic voltammetry, confirm this behavior.

0947-6539/99/0502-0660 $ 17.50+.50/0 *Chem. Eur. J.* **1999**, *5*, No. 2

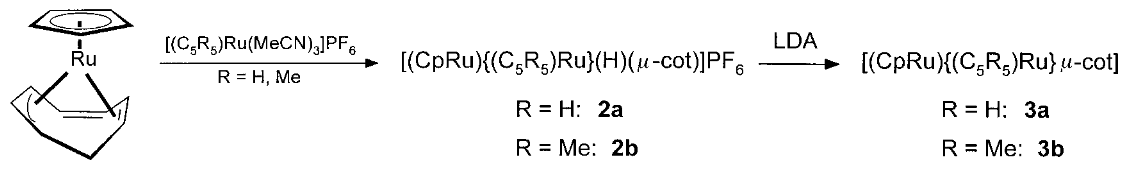

1

Scheme 3. Formation of the dinuclear hydridoruthenium complexes **2a** (R = H) and **2b** (R = Me) and conversion to **3a** and **3b**.

The cyclic voltammogram of **3a** (Figure 1, Table 1) shows two electrochemically reversible redox waves with an identical peak current. Thus, the waves can be assigned to the redox pairs 0/+1 (−0.79 V vs. $[FeCp_2]/[FeCp_2]^+$) and +1/+2 (−0.17 V vs. $[FeCp_2]/[FeCp_2]^+$). The corresponding potentials of **3b** are cathodically shifted by 100 mV; this is not unexpected because of the inductive effect of the additional five methyl groups in comparison to **3a**.[2a,b] The results of the redox study of our diruthenium cyclooctatetraene complexes are in sharp contrast to the redox properties known for the *antifacial* $[(CpRu)_2\mu\text{-cot})]$ complex, which reveals an electrochemically irreversible, two-electron oxidation.[4b]

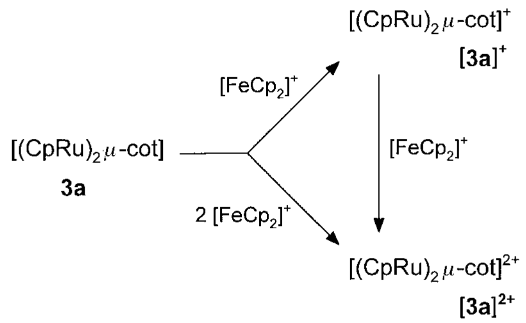

Scheme 4. Oxidation of **3a** by ferrocenium cation.

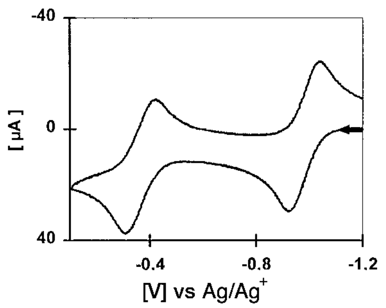

Figure 1. Cyclic voltammogram of **3a** ($\nu = 100\ mV\,s^{-1}$, see text).

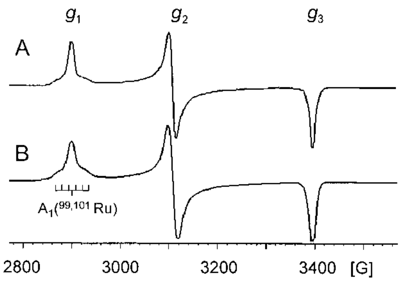

Figure 2. EPR spectra of $[3a]^+$; (A) experimental spectrum, $T = 100$ K; (B) calculated spectrum.

Table 1. Cyclic voltammetry data[a] of **3a** and **3b**.

	i_{pc}/i_{pa}	$E_{1/2}$ (0/+1)[b] [V]	ΔEp[c] [mV]	i_{pc}/i_{pa}	$E_{1/2}$(+1/+2)[b] [V]	ΔEp[c] [mV]	ΔE[d] [V]
3a	1.05	−0.791	108	1.05	−0.174	102	0.62
3b	1.05	−0.892	114	1.03	−0.267	108	0.62

[a] $\nu = 100\ mV\,s^{-1}$. [b] +0.005 V vs. $[FeCp_2]/[FeCp_2]^+$. [c] $\Delta Ep([FeCp_2]/[FeCp_2]^+) = 130$ mV. [d] $\Delta E = E_{1/2}(+1/+2) - E_{1/2}(0/+1)$.

Since both oxidation potentials of **3a** are considerably more negative than those of ferrocene, **3a** can be preparatively oxidized with ferrocenium cation to the monocation $[3a]^+$ or even the dication $[3a]^{2+}$ when the required amount of $[FeCp_2]^+$ is taken into account (Scheme 4).

The monocation $[3a]^+$ is paramagnetic with one unpaired electron. An EPR spectrum of $[3a]^+$ can only be obtained from solid solution (Figure 2 A) and shows the fine structure of a rhombic g tensor ($g_1 = 2.3217(5)$, $g_2 = 2.1642(5)$, $g_3 = 1.9818(5)$) with the pronounced anisotropy of a metal-centered radical. The low-field signal at $g_1 = 2.3217$ is superimposed with a broad signal of lower intensity caused by an unresolved Ru hyperfine coupling.[10] The best fit for the experimental EPR spectrum is obtained when the natural abundances of the magnetically active Ru isotopes are doubled (Figure 2 B), proving a complete delocalization of the unpaired electron on both of the metal centers.

Because of the time scale of EPR spectroscopy, it is impossible to discriminate between a mixed-valent class II or class III compound in this case.[11] Therefore UV/Vis spectroscopic studies were performed (Figure 3), from which it was concluded that the cation $[3a]^+$ is a mixed-valent compound

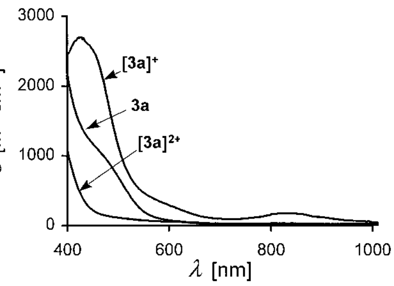

Figure 3. UV/Vis spectra of **3a**, $[3a]^+$ (in CH_2Cl_2) and $[3a]^{2+}$ (in $MeNO_2$)

of class III: a long-wave absorption band at $\lambda_{max} = 830$ nm of low intensity ($\varepsilon = 150\ M^{-1}cm^{-1}$) is only observed for the monocation and its position is insignificantly influenced by the polarity of the solvent; additionally, the half-width of this signal ($\Delta\nu_{1/2} = 2530\ cm^{-1}$) is less than half of the value calculated according to Hush[12] ($\Delta\nu_{1/2}$ (calcd) = $(2310 \times \nu_{max})^{1/2}$ = 5275 cm^{-1}). These results indicate that the electronic excitation at λ = 830 nm is caused by an intervalence transition. The mixed-valent class III for $[\mathbf{3a}]^+$ is also corroborated by the large comproportionation constant $K_c > 3 \times 10^{10}$, which can be estimated from the difference of the two oxidation potentials ΔE of **3a** and **3b**.[13]

The almost identical separation of the two oxidation potentials in **3a** and **3b** can be taken as an additional argument for a SOMO which incorporates both Ru centers equally: if the two electrons are removed stepwise from two orbitals located at different metal centers, the permethylation of one cyclopentadienyl ligand would be expected to induce a different influence on the two oxidation potentials.

Important indications of the structural arrangements of the four complexes under study can be deduced from NMR spectroscopic data (Table 2). Temperature-dependent

Table 2. ^{1}H and ^{13}C NMR data of the homodinuclear Ru complexes **2a**, **2b**, **3a**, **3b** and $[\mathbf{3a}]^{2+}$.

2a: ^{1}H NMR[a] (295 K): δ = 5.62 (s, 10H, Cp), 4.56 (s (broad), 8H, cot), −16.94 (s, 1H, Ru-H); ^{1}H NMR[a] (200 K): δ = 5.62 (s, 10H, Cp), 4.69 (m, 4H, cot), 4.39 (m, 4H, cot), −17.14 (s, 1H, Ru-H); ^{13}C NMR[b] (300 K): δ = 83.76 (Cp), 83.7 (cot).

2b: ^{1}H NMR[a] (295 K): δ = 5.51 (s, 5H, Cp), 4.10 (s (broad), 8H, cot), 2.0 (s, 15H, C_5Me_5), −17.18 (s, 1H, Ru-H); ^{1}H NMR[a] (220 K): δ = 5.51 (s, 5H, Cp), 4.54 (m, 2H, cot), 4.32 (m, 2H, cot), 4.03 (m, 2H, cot), 3.61 (m, 2H, cot), 2.0 (s, 15H, C_5Me_5), −17.25 (s, 1H, Ru-H); ^{13}C NMR[b] (300 K): δ = 97.8 (C_5Me$_5$), 83.1 (Cp), 10.5 (C$_5$*Me*$_5$).

3a: ^{1}H NMR[c]: δ = 4.76 (s, 5H, Cp), 4.06 (s, 4H, cot); ^{13}C NMR[d]: δ = 76.4 (Cp), 55.7 (cot).

3b: ^{1}H NMR[c]: δ = 4.77 (s, 5H, Cp), 3.57 (s, 8H, cot), 1.63 (s, 15H, C_5Me_5); ^{13}C NMR[d]: δ = 87.5 (C_5Me$_5$), 74.9 (Cp), 57.7 (cot), 10.5 (C_5Me_5).

$[\mathbf{3a}]^{2+}$**:** ^{1}H NMR[e] (353 K): δ = 6.3 (s, Cp), 5.5 (s (broad), cot); ^{1}H NMR[e] (230 K): δ = 6.29 (s, 5H, Cp), 8.01 (s (broad), 1H, cot), 5.99 (s (broad), 2H, cot), 1.72 (s (broad), 1H, cot).

[a] 360 MHz, [D$_6$]acetone, rel. TMS. [b] 50 MHz, [D$_6$]acetone, rel. TMS. [c] 360 MHz, [D$_6$]benzene, rel. TMS. [e] 360 MHz, [D$_3$]nitromethane, rel. [D$_2$]nitromethane δ = 4.32.

^{1}H NMR spectra of **2a** and **2b** reveal sharp singlets for the Cp and Cp* protons at all temperatures, whereas the cot protons show one broad signal at ambient temperature, but two and four multiplets, respectively, on cooling (Figure 4). For **2a**, an activation barrier of 37 kJ mol^{-1} can be estimated from a line shape analysis.[14] This is appreciably lower than that for the antifacial congeners [(CpRu)$_2\mu$-cot] and [(CpRh)$_2\mu$-cot]$^{2+}$, where the cot ligand shows a sharp singlet distinctly above 300 K.[4a, 15] Temperature dependence of the ^{1}H NMR spectra comparable to **2a** is reported for dinuclear synfacial μ-cycloheptatrienyl complexes which contain two metal centers bridged by a hydrogen atom.[9]

Similar to the dinuclear μ-cycloheptatrienyl μ-hydrido complexes,[9] an additional high-field resonance line for **2a** and **2b** was recorded at −16.94 and −17.18 ppm, respectively, with the intensity of one proton. The high-field shift is typical for a bridging hydrogen in a dinuclear Ru complex.[16] Apparently C−H activation has occurred during the formation of the dinuclear complexes **2a** and **2b**, which leads to a symmetrical coordination of the hydrogen atom between the two Ru centers, at least in **2a** with respect to the NMR time scale.

Upon deprotonation, the cot ligand in **3a** and **3b** reveals a sharp singlet at T = 180 K only, which suggests the ligand is still undergoing fast rotation, even at such a low temperature. The fluxional behaviour with a low energy-to-rotation is well known for synfacially coordinated dinuclear μ-cot complexes with 34 ve,[4a, 17, 18] whereas the antifacial stereoisomer of [(CpRu)$_2\mu$-cot] exhibits, besides the Cp resonance, four broad proton lines at ambient temperature, which resolve on cooling.[4b]

In conclusion, our NMR results indicate the synfacial coordination of the two cyclopentadienyl ruthenium moieties bound in a η^4:η^4 fashion to the cot ligand, at least in the protonated forms **2a** and **2b**. The two sets of signals for the cot ligand in **2a** are a consequence of the local C_{2v} symmetry of the Ru$_2$(μ-cot) fragment. The symmetry lowers to C_s when one Cp ligand is permethylated, and gives rise to four different sets of protons (Table 2).

A synfacial coordination mode is also in agreement with the ^{1}H NMR spectra of the dication $[\mathbf{3a}]^{2+}$. At room temperature only the singlet of the Cp protons can be observed. When the temperature is lowered, three different unresolved signals appear at δ = 8.01, 5.99, and 1.72 with an intensity ratio of 1:2:1. The intensity ratio and the strong high-field shift of one of the cot signals are well known from the electron-poor, synfacial 28 ve complex [(CpV)$_2\mu$-cot] with a η^5:η^5 bonding mode of the cot ligand.[2d, 19] Hence, a synfacial η^5:η^5 coordination mode is also evident for $[\mathbf{3a}]^{2+}$. The structural features deduced from the NMR spectroscopic results can be fully verified by X-ray structure analysis.

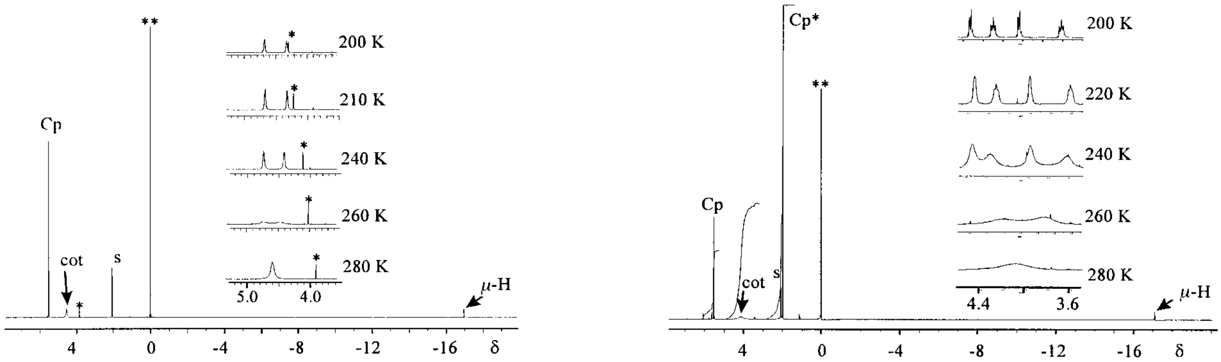

Figure 4. Temperature-dependent ^{1}H NMR spectra of **2a** (left), and **2b** (right) (* = impurity, ** = TMS, s = [D$_8$]toluene).

X-Ray structure analysis and bonding: X-ray structure analysis has been performed on all diruthenium complexes presented here to allow a deeper insight into the structural changes and bonding associated with the variation of charge. As shown by Ru–C distances and the C–C bond lengths within the metal-coordinated diene units, **2a** (Figure 5) and **3a** (Figure 6) comprise a synfacial η^4:η^4 bonding mode of the cot moiety; this is in agreement with the NMR results for **2a** in solution. Each η^4-diene unit interacts with one Ru center, to form two long and two short bonds for the proximal and distal Ru–C(cot) bonds, respectively, a feature normally found in dinuclear η^4:η^4-cot complexes.[4a, 17, 18] The C–C bond lengths within a η^4-diene unit are considerably shorter than the C–C bond which links the two η^4-diene moieties, thus reducing the π interaction between them.

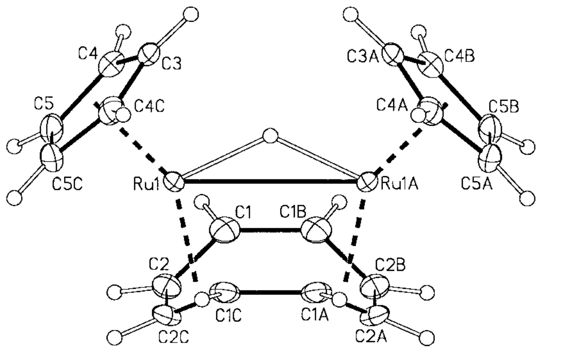

Figure 5. Molecular structure of **2a** (ORTEP, 50% thermal ellipsoids, the anion PF_6^- is omitted for clarity). Selected bond lengths [pm] and angles [°]: Ru1–Ru1A 307.75(8), C1–C2 141.8(2), C2A–C2C 142.8(4), C1–C1B 145.8(3), Ru–C1 221.9(2), Ru–C2 216.6(2), Ru–C3 222.7(2), Ru–C4 222.2(2), Ru–C5 217.8(2), Ru–H 173(2); Ru-H-Ru 126, plane(C1-C2-C2C-C1C) – plane(C1A-C2A-C2B-C1B) 107.6(9), plane(Cp1) – plane(Cp2) 90.3(10), plane(C1-C2-C2C-C1C) – plane(Cp) 8.6(9).

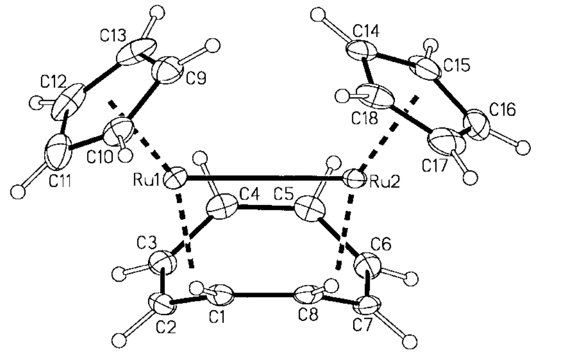

Figure 6. Molecular structure of **3a** (ORTEP, 50% thermal ellipsoids). Selected bond lengths [pm] and angles [°]: Ru1–Ru2 295.6(1), C1–C2 142.8(4), C1–C8 145.5(4), C2–C3 142.8(5), C3–C4 143.0(5), C4–C5 145.0(5), C5–C6 142.4(5), C6–C7 142.5(5), C7–C8 142.6(5), Ru1–C1 220.6(3), Ru1–C2 215.7(3), Ru1–C3 216.3(3), Ru1–C4 222.8(3), Ru2–C5 221.5(3), Ru2–C6 216.4(3), Ru2–C7 216.1(3), Ru2–C8 221.4(3) Ru1–C9 225.1(4), Ru1–C10 222.9(3), Ru1–C11 217.6(4), Ru1–C12 217.9(4), Ru1–C13 222.4(4), Ru2–C14 221.8(3), Ru2–C15 223.2(3), Ru2–C16 220.4(4), Ru2–C17 220.3(4); plane(C1 – C4) – plane(C5 – C8) 113.3(2), plane(Cp1) – plane(Cp2) 109.1(1), plane(C1 – C4) – plane(Cp1) 4.9(3), plane(C5 – C8) – plane(Cp2) 0.8(4) (Cp1 = C9 – C13, Cp2 = C14 – C18).

An important result of the X-ray structure analysis of **2a** was the location of a bridging hydrogen atom from the residual electron density. The hydrogen atom is equidistant from the two Ru atoms (Ru – H 173(2) pm), a fact which seems to be unusual for a hydrogen atom bridging two Ru centers;[20] even in the symmetrically substituted Ru_2 complex $[(Cp_2CH_2)Ru_2(CO)_4\mu\text{-H}]^+$, a nonsymmetric coordination of the μ-H is found.[16] Interestingly, the average of the Ru–H bond lengths in $[Cp_2CH_2Ru_2(CO)_4(\mu\text{-H})]^+$ is equal to the Ru–H bond length in **2a**. This correlation could lead to the suggestion that the symmetrical hydrogen bridge is merely simulated. Although this cannot be totally excluded in such cases, there is no further evidence that would confirm statistical disorder or dynamic behavior such as a hydrogen atom hopping between the two metal centers. The bonding of the RuHRu group is best described as a three-center, two-electron bond which grants each Ru center an 18 ve configuration.[21]

A characteristic of hydrido-bridged bimetallic complexes is the decrease of the intermetallic distance upon deprotonation,[16, 22] as exemplified when **2a** is deprotonated to **3a**. The Ru–Ru distance decreases to 295.6 pm in **3a** and is almost identical to the length of the Ru–Ru bond in the dicationic dinuclear ruthenocenophane, which has been proven to contain a true Ru–Ru bond that keeps the metal centers in close contact.[23] A Ru–Ru single bond in **3a** provides an 18 ve configuration for each Ru center. Therefore, the two C_4H_4Ru fragments of the $Ru_2(\mu\text{-cot})$ moiety coordinatively act as cyclopentadienyl ligands: the Ru atom of a C_4H_4Ru unit takes the place of a C atom of the second Cp ligand of the neighboring metallocene to form a fused bimetallocene which we call twinnocene (here: Ru – Ru twinnocene).[2c, 24]

The structural changes that occur from **2a** to **3a** give a clue to the different temperature dependences of the cot ligands observed by ^{1}H NMR spectroscopy. Whilst the C–C and Ru–C bond lengths in **2a** and **3a** do not differ significantly, the angle between the two planes formed by the η^4-coordinated butadiene moieties becomes less acute upon reduction of the Ru–Ru distance: 107.6(9)° in **2a** compared to 113.3(2)° in **3a**. Consequently, the bridging *cyclo*-C_8 ligand in **3a** needs less energy to flatten, which makes the cot ligand easier to rotate.

The oxidation of **3a** to [**3a**]$^+$ changes the hapticity of the cot ligand and [**3a**]$^+$ adopts a η^5:η^5 bonding mode (Figure 7). At the same time, the Ru–Ru distance decreases to 282 pm. Upon further oxidation to [**3a**]$^{2+}$, the coordination mode of the $Ru_2(\mu\text{-cot})$ entity remains unchanged, whereas a distinct contraction of the intermetallic distance to 266 pm takes place accompanied with a decrease of the distance of the Ru centers to the bridging carbon atoms C1 and C5 of the cot ligand from 243 – 246 pm to 237 pm (Figure 8). In contrast, the Ru distances to the Cp carbon atoms and to the C atoms of the cot moiety, excluding the bridging C atoms, scarcely vary upon oxidation from [**3a**]$^+$ to [**3a**]$^{2+}$.

The cot ligand in [**3a**]$^+$ and [**3a**]$^{2+}$ consists of the two virtually planar pentadienyl units that enclose an interplanar angle of 130.9 and 129° for the two different molecules in the unit cell of [**3a**]$^+$, and of 127.5° for [**3a**]$^{2+}$. These angles fall into the range of values known for other dinuclear complexes with a μ-(η^5:η^5) bonding mode of the cot moiety which extends from 124° to 138°.[2d, 3, 19, 25, 26] Similar to the rotational barrier

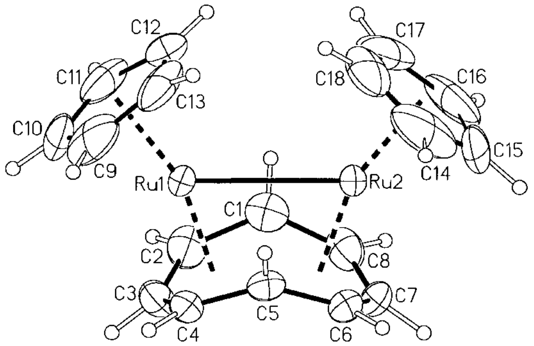

Figure 7. Molecular structure of [**3a**]PF_6 (ORTEP, 30% thermal ellipsoids; the anion PF_6^- is omitted for clarity). A second, independent molecule in the unit cell, which is not shown, contains a molecular C_2 axis; however, the bond lengths and angles are very similar to the molecule shown in this figure. Selected bond lengths [pm] and angles [°] for the molecule shown above: C1–C8 143.0(10), C1–C2 144.3(10), C2–C3 140.8(10), C3–C4 137.0(10), C4–C5 146.1(9), C5–C6 144.2(9), C6–C7 139.1(11), C7–C8 138.8(10), Ru1–Ru2 282.15(9), Ru1–C4 213.9(6), Ru1–C2 215.5(6), Ru1–C3 217.0(6), Ru1–C5 242.9(6), Ru1–C1 246.3(6), Ru2–C6 214.4(6), Ru2–C8 215.6(6), Ru2–C7 216.3(6), Ru2–C5 245.9(6), Ru2–C1 246.0(6), Ru1–C9 217.9(5), Ru1–C10 216.1(5), Ru1–C11 218.5(5), Ru1–C12 221.8(5), Ru1–C13 221.5(5), Ru2–C14 220.1(5), Ru2–C15 216.5(5), Ru2–C16 217.1(5), Ru2–C17 221.2(5), Ru2–C18 223.0(4); plane(C1–C5)–plane(C1-C5-C6-C7-C8) 130.9(4), plane(Cp1)–plane(Cp2) 103.0(8), plane(C1–C5)–plane(Cp1) 13.3(6), plane(C1-C5-C6-C7-C8)–plane(Cp2) 14.7(6) (Cp1 = C9–C13, Cp2 = C14–C18).

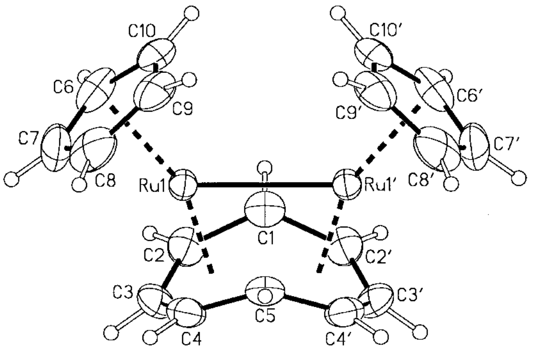

Figure 8. Molecular structure of [**3a**](BF_4)(PF_6) (ORTEP, 30% thermal ellipsoids; the anions BF_4^- and PF_6^- are omitted for clarity). Selected bond lengths [pm] and angles [°]: C1–C2 142.2(5), C2–C3 139.3(7), C3–C4 139.4(7), C4–C5 143.4(5); Ru1–Ru1′ 266.08(6), Ru–C1 236.9(5), Ru–C2 212.5(4), Ru–C3 216.2(4), Ru–C4 213.0(4), Ru–C5 238.0(4), Ru–C6 216.0(4), Ru–C7 216.5(5), Ru–C8 216.8(4), Ru–C9 220.7(4), Ru–C10 220.5(4); plane(C1-C5)-plane(C1C2′C3′C4′C5) 127.5(3), plane (Cp)-plane (Cp′) 99.2(5), plane(C1-C5)-plane(Cp) 14.0(4).

of the η^4:η^4-bound cot ligand, there is an evident correlation between the interplanar angle of the two η^5-C_5 planes of the cot ligand and its energy barrier of rotation. The rotational barrier drops in the order of increasing interplanar angle: [$(CpV)_2\mu$-cot] (123.8°)[19] > [$(CpRu)_2\mu$-cot]$^{2+}$ (127.5°) > [$(CpCr)_2\mu$-cot] (131.2°),[19] [$Cr_2(cot)_3$] (132°),[25] [(CpFe)(CpCo)μ-cot]$^+$ (138°).[3]

A typical feature of the η^5:η^5 bonding mode is the distinct elongation of the C–C bonds attached to the μ-carbon atoms, with respect to the other carbon–carbon bond lengths of the cot ligand. Hence, the bonding of the two bridging carbon atoms C1 and C5 of [**3a**]$^{2+}$ is most simply described by the two resonance forms, A and B. Compound [**3a**]$^{2+}$ is composed of two bent sandwich complexes fused by two bridging carbon atoms of the C_5H_5 subunit of the cot ligand and by a Ru–Ru single bond which provides an 18 ve configuration for a Ru atom in each resonance form (Scheme 5).

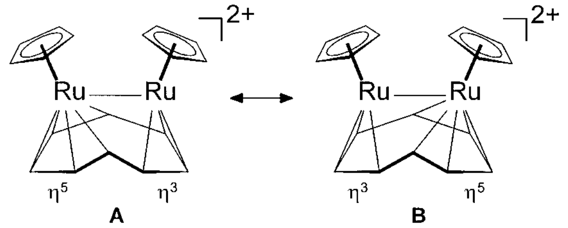

Scheme 5. Resonance forms of [**3a**]$^{2+}$

The classification of a Ru–Ru single bond in [**3a**]$^{2+}$ is not only justified by the short Ru–Ru distance of 266 pm, but also agrees with the concept of the qualitative MO picture sketched for the direct metal–metal interaction in electron-deficient complexes of the general composition [(CpM)(CpM′)μ-(η^5:η^5-cot)] (M, M′ = V, Cr).[2d] The individual frontier orbitals of the two $CpMC_5H_5$ sandwich units in [(CpM)(CpM′)μ-(η^5:η^5-cot)], which must be considered for a direct intermetallic contact, are derived from MOs of bent metallocenes.[26] The metal-based frontier orbitals are $1a_1$-, b_2- and $2a_1$ and their combination gives rise to σ-, π- and δ-type orbitals. For M = M′ = V, these orbitals are doubly occupied, albeit the δ bond is very weak, which brings about a thermal population of the δ* orbital resulting in a singlet–triplet equilibrium (Figure 9).[2d] The 30 ve complex [$(CpCr)_2\mu$-cot]

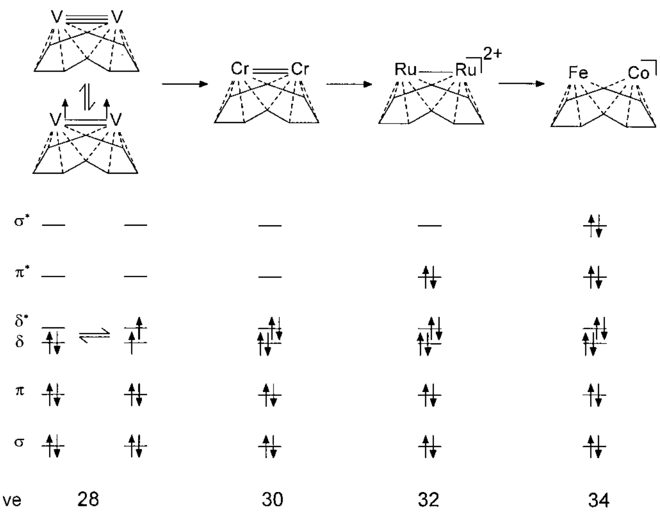

Figure 9. Population of the σ-, π- and δ-type orbitals in [(CpM)(CpM′)μ-(η^5:η^5-cot)]^n (n = −1, 0, +1, +2) which are responsible for the direct metal–metal interaction (compare Ref. [2d], Cp ligands in the formulae are omitted for clarity).

is purely diamagnetic with the population of σ^2 π^2 δ^2 δ^{*2}, which represents a formal Cr–Cr double bond. In the 32 ve complex [**3a**]$^{2+}$ the π*orbital is additionally filled, which leads to a metal–metal single bond. In this series a corresponding 34 ve complex would be expected to have a doubly occupied σ* orbital and would not have a metal–metal bond. This case is avoided by the Ru_2 entity, as seen above, and a η^4:η^4

  0947-6539/99/0502-0664 $ 17.50+.50/0 *Chem. Eur. J.* **1999**, *5*, No. 2

coordination mode is adopted, which again results in a Ru–Ru single bond.

Interestingly, the behavior of metal centers kept in close proximity to maintain a metal–metal bond was reported for synfacially coordinated [(CpRh)$_2\mu$-cot]:[4a] the cot ligand was then bound in a η^3:η^3 fashion, which left one double bond of the cot free and the Rh–Rh distance was 268.9(1) pm, very similar to the Ru–Ru bond length in [**3a**]$^{2+}$, which is a strong indication for a metal–metal single bond. An alternative coordination mode would have been a synfacial η^4:η^4 cot linkage without a Rh–Rh bond, which is apparently not formed.

However, a synfacial η^5:η^5 coordination mode without a metal–metal bond was observed in the heterodinuclear 34 ve cation [(CpFe)(CpCo)μ-cot)]$^+$, in which a Fe–Co single bond can be excluded in view of the long Fe–Co distance (>286 pm).[3] It is reasonable to assume that direct Fe–Co bond formation is unfavorable because the metal orbitals which are responsible for the direct intermetallic communication will be too different in energy for formal Fe^{II} and Co^{III} centers. EPR studies of heterodinuclear μ-cot complexes substantiate this assumption. In the case of paramagnetic heterodinuclear μ-cot complexes, a predominant localization of unpaired electrons on one metal center is recognized, whereas delocalization occurs in homodinuclear congeners.[2a–d]

Furthermore, the EPR results of the 29, 31[2d] and 33 ve species corroborate this qualitative MO picture: the large metal hyperfine coupling constants, the distinct deviation of the isotropic g value from $g_e = 2.0023$ (g value of the free electron) and the pronounced g anisotropy in magnetically diluted solid-state spectra confirm the metal-centered nature of the unpaired electron. The latter, in particular, is true for [**3a**]$^+$, which has been shown to be a mixed-valent class III compound.

With the synthesis of the new *synfacial* diruthenium complexes [**3a**]$^+$ and [**3a**]$^{2+}$, the series of μ-(η^5:η^5)-cot complexes of the general type [(CpM)(CpM′)μ-(η^5:η^5-cot)]$^{n+}$ ($n = -1, 0, +1, +2$) is completed in the range 28 to 34 ve, for which a concise although qualitative MO concept with respect to the metal–metal bond could be developed.[24]

Conclusions

Synfacially coordinated μ-cot diruthenium complexes can be synthesized straightforwardly from [CpRu(1,2,3-η:6,7-η-C_8H_9)] and [(C_5R_5)Ru(MeCN)$_3$]PF_6 (R = H, Me) as the starting materials. At first the cationic μ-hydrido complexes [(CpRu){(C_5R_5)Ru}(μ-H)(μ-cot)]PF_6 (R = H: **2a**; R = Me: **2b**) are formed, then deprotonation affords the desired synfacial isomers (**3a**, **3b**) of the known antifacial species [(CpRu)$_2\mu$-cot].[4a, 4b] Complexes **3a** and **3b** undergo two electrochemically reversible one-electron oxidations at ambient temperature, whereas the antifacial isomer is subjected to an electochemically irreversible two-electron oxidation involving the cleavage of a C–C bond in the cot ligand.[4b]

The oxidation of **3a** reveals a change in hapticity of the cot ligand as shown by X-ray structure analysis: in **2a** and **3a**, the cot ligand is bound in a η^4:η^4 fashion and transforms to a η^5:η^5 bonding mode upon oxidation of **3a**. Simultaneously, the Ru–Ru distance decreases continuously from 307.8 pm in the μ-hydrido complex **2a** to 266 pm in [**3a**]$^{2+}$. Interestingly, despite the same formal Ru–Ru bond order of one in **3a** as well as in [**3a**]$^{2+}$, the metal–metal bond length of the latter is about 30 pm shorter than in **3a**. This example highlights the importance of the oxidation state of the metal centers for the metal–metal bond length variance with respect to a particular bond order.

The present study and a comparison of structural results of other synfacially coordinated dinuclear μ-cot complexes offer an explanation for the change of the hapticity of the μ-cot moiety, which appears to be correlated to the metal–metal distance: in [{$Mn_2(CO)_6$}μ-cot],[27] [{$Ru_2(CO)_5$}μ-cot],[18] [(CpRu)$_2$(μ-H)(μ-cot)]$^+$ and [(CpRu)$_2\mu$-cot] which contain intermetallic distances of more than 290 pm, a η^4:η^4 bonding mode is found, whereas in [{$Fe_2(CO)_5$}μ-cot],[28] [(CpRu)$_2\mu$-cot]$^{n+}$ ($n = 1, 2$), [(CpFe)(CpCo)μ-cot]$^+$,[3] [(CpM)$_2\mu$-cot] (M = V, Cr)[19] in which the metal–metal distance is less than 290 pm, all have the cot entity bound in a η^5:η^5 fashion.

Another remarkable feature of the synfacially constructed dinuclear μ-cot complexes is the urge of homometal complexes to form metal–metal bonds, whereas heterometal complexes tend to avoid metal–metal bonds if the electronic requirement can be sufficiently fulfilled by structural rearrangements, as can be seen for [(CpRu)$_2\mu$-(η^5:η^5-cot)]$^{2+}$ and [(CpRu)$_2\mu$-(η^4:η^4-cot)] as well as for [(CpRh)$_2\mu$-(η^4:η^4-cot)]$^{2+}$ and [(CpRh)$_2\mu$-(η^3:η^3-cot)].[4a] The cationic complex [(CpFe)(CpCo)μ-(η^5:η^5-cot)]$^+$ is electronically isovalent to [(CpRu)$_2\mu$-(η^4:η^4-cot)], but has a different cot bonding mode and shows no indication of a metal–metal bond. If a Fe–Co bond is formed, a η^4:η^4 bonding mode of the cot ligand would be required by electron bookkeeping in this complex.

The difference in intermetallic communication of homo- and heterodinuclear μ-cot complexes is also manifested in spectroscopic results, namely EPR spectroscopy of congeners with an odd numer of electrons. Paramagnetic homodinuclear species, even on the UV/Vis time scale reveal complete delocalization, whereas heterodinuclear complexes show predominant localization of the unpaired electron on one metal center.

The bonding in **2a** and **3a** can be described as the fusion of two ruthenocenes, where a Ru center of a metallocene unit takes the place of a carbon atom of one Cp ligand from the other metallocene. The metal–metal interaction in [**3a**]$^{2+}$ and [**3a**]$^+$ is interpreted as follows: in accordance with other dinuclear μ-(η^5:η^5-cot) complexes,[2d] the proposed population of the orbitals responsible for metal–metal interaction in [**3a**]$^{2+}$ and [**3a**]$^+$ is $\sigma^2\ \pi^2\ \delta^2\ \delta^2\ \pi^{*2}$ and $\sigma^2\ \pi^2\ \delta^2\ \delta^{*2}\ \pi^{*2}\ \sigma^{*1}$ (see Figure 9), respectively, which results in a Ru–Ru single bond in [**3a**]$^{2+}$ and a semi-occupied σ* type MO in [**3a**]$^+$.

Experimental Section

Manipulations were carried out under a N_2 atmosphere and solvents were saturated with N_2. THF, Et_2O, DME, hexane, and toluene were freshly distilled from the appropriate alkali metal or metal alloy; $MeNO_2$ was dried over CaH_2 and distilled under N_2. NMR: Bruker AM 360; UV/Vis: Perkin-

Elmer Model 554; IR: nujol null, KBr cells, FT-IR 1720X (Perkin Elmer); EI-MS: 70 eV, Finnigan MAT 311 A; elemental analysis: Heraeus CHN-O-Rapid, Institut für Anorganische und Angewandte Chemie, Universität Hamburg. Complexes $[CpRu(\eta^6\text{-cot})]PF_6$, $[CpRu(MeCN)_3]PF_6$, and $[Cp^*Ru(MeCN)_3]PF_6$ were synthesized by literature methods.[7a, 7b]

(1,2,3-η:6,7-η-Cyclooctatrienyl)(η^5-cyclopentadienyl)ruthenium (1): $Li[BEt_3H]$ (4.97 mL; 1.0 M in THF) was added to a cooled (220 K), stirred suspension of $[CpRu(\eta^6\text{-cot})]PF_6$ (2.06 g, 4.95 mmol) in THF (50 mL). The mixture was allowed to warm to room temperature. After stirring for 1 h, the reaction mixture was evaporated to dryness, the residue was extracted with hexane, and the hexane solution was filtered through kieselgel. The solvent was removed and the yellow oily residue thoroughly dried in vacuum. Yield: 1.34 g (99%). IR (Nujol, KBr): $\tilde{\nu} = 1645\,cm^{-1}$ (C=C). ^1H NMR (360 MHz, C_6D_6, rel. TMS, 297 K): $\delta = 4.40$ (s, 5H, Cp), 2.65 (m, 1H, 1-H), 3.96 (dd, $^3J_{1,2} = 7.5$ Hz, $^3J_{2,3} = 2.1$ Hz, 1H, 2-H), 5.46 (dd, $^3J_{3,4} = 6.1$ Hz, 1H, 3-H), 5.54 (dd, $^3J_{4,5} = 3.2$ Hz, 1H, 4-H), 4.57 (dd, $^3J_{5,6} = 7.5$ Hz, 1H, 5-H), 3.18 (dd, $^3J_{6,7} = 7.5$ Hz, 1H, 6-H), 3.33 (m, 1H, 7-H), 2.87 (m, 2H, 8_{endo}-H, 8_{exo}-H); $^{13}C\{^1H\}$ NMR (50 MHz, C_6D_6, rel. TMS, 297 K): $\delta = 79.6$ (Cp), 12.4 (C-1), 66.8 (C-2), 135.0 (C-3), 132.3 (C-4), 63.4 (C-5), 74.2 (C-6), 21.7 (C-7), 22.6 (C-8). EI-MS: *m/z* (%): 271 (93) $[M^+ - H]$; $C_{13}H_{14}Ru$: calcd C 57.55, H 5.20; found C 57.57, H 5.30.

[{μ-(1,2,3,4-η:5,6,7,8-η)Cyclooctatetraene}bis(η^5-cyclopentadienyl)(μ-hydrido)diruthenium] hexafluorophosphate (2a): Solid $[(C_5H_5)Ru(MeCN)_3]PF_6$ (2.00 g, 4.61 mmol) was added to a solution of **1** (134 g, 4.95 mmol) in CH_2Cl_2 (80 mL). After stirring for 4 h, the red reaction mixture was filtered to afford **2a** as an orange-red crystalline material. Additional product was obtained by dilution of the filtrate with Et_2O. Yield: 1.99 g (98%). IR (Nujol): $\tilde{\nu} = 3122$ w, 3064 w, 1598 m, 1426 w, 1407 m, 1012 m, 958 m, 854 s (PF_6), 740 m, 558 s cm^{-1}; EI-MS: *m/z* (%): 435 (0.5) $[M^+ - PF_6]$, 271 (10) $[RuCpC_8H_8^+]$, 232 (100) $[RuCp_2^+]$, 167 (44) $[RuCp^+]$; $C_{18}H_{19}F_6PRu_2$: calcd C 37.12, H 3.29; found C 36.49, H 3.40.

[{μ-(1,2,3,4-η:5,6,7,8-η)Cyclooctatetraene}(η^5-pentamethylcyclopentadienyl)(η^5-cyclopentadienyl)(μ-hydrido)diruthenium] hexafluorophosphate (2b): The reaction was carried out as for **2a**: **1** (0.254 g, 0.94 mmol), CH_2Cl_2 (15 mL), $[Cp^*Ru(MeCN)_3]PF_6$ (448 mg, 0.89 mmol). Yield: 398 mg (69%) of **2b**. MS (FABS): 508 (100) $[M - PF_6]$; EI-MS: *m/z* (%): 302 (100) $[RuCpCp^{*+}]$, 287 (88) $[RuCpC_5Me_4^+]$, 271 (20) $[RuCpC_8H_8^+]$, 232 (60) $[Ru\ Cp_2^+]$, 169 (100) $[RuCp^+]$; $C_{23}H_{29}F_6PRu_2$: calcd C 42.33, H 4.48; found C 41.26, H 4.43.

[μ-(1,2,3,4-η:5,6,7,8-η)Cyclooctatetraene)]bis(η^5-cyclopentadienyl)diruthenium (*Ru–Ru*) (3a): A solution of LDA (0.45 mL, 2 M) in THF/heptane/ethylbenzene (Merck) was slowly added to a suspension of **2a** (262 mg, 0.45 mmol) in THF (40 mL). After 2 h, the reaction suspension was evaporated to dryness, the residue extracted with toluene, and the orange-colored toluene solution was filtered through kieselgel. The solvent was removed in vacuo and the residue dissolved in hexane . After cooling the mixture (−40 °C), **3a** precipitated as a red crystalline material. Yield: 190 mg (97%). $C_{18}H_{18}Ru_2$: calcd C 49.53, H 4.16; found C 49.10, H 5.01.

[μ-(1,2,3,4-η:5,6,7,8-η)Cyclooctatetraene](η^5-pentamethylcyclopentadienyl)(η^5-cyclopentadienyl)diruthenium (*Ru–Ru*) (3b): The reaction was carried out as for **3a**: **2b** (239 mg, 0.37 mmol), THF (35 mL), LDA solution (0.37 mL, 0.74 mmol). Yield: 154 mg (81%). $C_{23}H_{28}Ru_2$: calcd C 54.53, H 5.57; found C 55.20, H 6.01.

[{μ-(1,2,3,4,5-η:1,5,6,7,8-η)Cyclooctatetraene}bis(η^5-cyclopentadienyl)diruthenium]hexafluorophosphate (*Ru–Ru*) ([3a]PF$_6$): Solid $[FeCp_2]PF_6$ (353 mg, 1.07 mmol) was added to a solution of **3a** (491 mg, 1.125 mmol) in CH_2Cl_2 (20 mL) and the reaction mixture was stirred for 1 h. After filtration, the reaction solution was evaporated to dryness, the residue washed several times with Et_2O, and dissolved in CH_2Cl_2. The green-brown CH_2Cl_2 solution was carefully layered with the same volume of Et_2O. After complete diffusion **[3a]**PF$_6$ was collected as a dark red-brown crystalline material. Yield: 432 mg (66%). $C_{18}H_{18}F_6PRu_2$: calcd C 37.18, H 3.12; found C 36.34, H 3.20.

[{μ-(1,2,3,4,5-η:1,5,6,7,8-η)Cyclooctatetraene}bis(η^5-cyclopentadienyl)diruthenium] bis(hexafluorophosphate) (*Ru–Ru*) ([3a](PF$_6$)$_2$): The reaction was carried out as for [**3a**]PF$_6$: **3a** (1 g, 2.3 mmol), CH_2Cl_2 (80 mL), $[FeCp_2]PF_6$ (1.52 g, 4.6 mmol) were dissolved in CH_2Cl_2 (100 mL). The green precipitate was collected and washed several times with CH_2Cl_2 until the filtrate was colorless. The dried residue was dissolved in a minimum amount of $MeNO_2$ and the product [**3a**](PF$_6$)$_2$ was precipitated by the addition of CH_2Cl_2. Yield: 722 mg (56%). $C_{18}H_{18}F_{12}P_2Ru_2$: calcd C 29.76, H 2.50, F 31.38, P 8.53; found C 27.08, H 2.61, F 29.10, P 7.75. [**3a**](PF$_6$)$_2$ decomposes slowly in solution and in the solid state, which is partially responsible for the unsatisfactory elemental analysis. The formation of $[CpRu(\eta^6\text{-cot})]^+$ could be observed as a decomposition product by ^1H NMR spectroscopy.

Cyclic voltammetry: An Amel System 5000 was used. The measurements were performed in DME with 0.4 M $[N(nBu)_4]ClO_4$ as supporting electrolyte, about 10^{-3} M solutions of **3a** and **3b**, a Pt wire as working electrode and a Pt plate (0.6 cm^2) as auxiliary electrode. The potentials are measured against Ag/Ag^+ and referenced against $E_{1/2}([FeCp_2]/[FeCp_2]^+) = 0$ V. The difference of the peak potentials was considerably larger than theoretically calculated, due to the solvent DME. Ferrocene and **3a**, **3b** show comparably large differences of the peak potentials.

EPR spectroscopy: The EPR spectra of [**3a**]$^+$ were obtained from oxygen-free $CHCl_3$:DMF (1:1) solutions at 100 K, and were recorded on a Bruker ESP 300e, X-band spectrometer. The calculations of the spectrum in Figure 2 were performed with the computer program Simfonia (Bruker). The fit parameters are: A_1 (^{99}Ru, ^{101}Ru) = 12 G, A_3 (^{99}Ru, ^{101}Ru) = 3.5, $W_1 = 14$ G, $W_2 = 16$ G, $W_3 = 9$ (W = line width), $g_1 = 2.3217$, $g_2 = 2.16415$, $g_3 = 1.9818$. Additionally, the contribution of ^{99}Ru and ^{101}Ru were taken into account with twice the natural abundance, leading to the relative proportions in the spectra of dinuclear complexes of 0.494 (I(Ru) = 0), 0.418 (I(Ru) = $1 \times 5/2$), 0.088 (I(Ru) = $2 \times 5/2$).

X-Ray structure analysis: Crystals of **2a** suitable for X-ray structure analysis were obtained by slow diffusion of Et_2O from the gas phase into a CH_2Cl_2 solution of **2a**. The same procedure was applied to obtain crystals of [**3a**]PF$_6$. Crystals of **3a** were obtained from hexane solution upon cooling. Crystals of [**3a**]$^{2+}$ precipitated after slow diffusion of a CH_2Cl_2 layer into a $MeNO_2$ solution of [**3a**](PF$_6$)$_2$. However, the only useable crystals for X-ray structure analysis were composed of a mixed BF_4/PF_6 salt. Apparently, the BF_4 anions must still have been present, perhaps as a BF_4^- impurity in the oxidant $[FcCp_2]PF_6$. Several attempts to prepare suitable crystals of the composition [**3a**](PF$_6$)$_2$ from pure **3a** and $[FeCp_2]PF_6$ failed. Only a microcrystalline green material was isolated. Crystallographic data for **2a**, **3a**, [**3a**]PF$_6$, [**3a**](BF$_4$)(PF$_6$) are given in Table 3.

Further details of the crystal structure investigation(s) can be obtained from the Fachinformationszentrum Karlsruhe, D-76344 Eggenstein-Leopoldshafen, Germany (fax: (+49) 7247-808-666; e-mail: crysdata@fiz-karlsruhe.de), on quoting the depository number CSD-410120 (**2a**), CSD-410187 (**3a**), CSD-410121 ([**3a**]PF$_6$), CSD-410122 [**3a**](BF$_4$)(PF$_6$).

Acknowledgements

This work was supported by the Deutsche Forschungsgemeinschaft (DFG, HE 1309/2). We are indepted to BASF for a donation of cyclooctatetraene and to DEGUSSA for a donation of $RuCl_3$.

[1] a) F. A. Cotton, R. A. Walton, *Multiple Bonds Between Metal Atoms,* 2nd ed., Clarendon Press, Oxford, **1993**; b) M. J. Winter, *Adv. Organomet. Chem.* **1989**, *29*, 101–162; c) T. Brauns, C. Carriedo, J. S. Cockayne, N. G. Conelly, G. G. Herbosa, M. G. Orpen, *J. Chem. Soc. Dalton Trans*, **1989**, 2049–2059.

[2] a) G. Bögels, H. C. Brussaard, U. Hagenau, J. Heck, J. Kopf, J. G. M. van der Linden, A. Roelofsen, *Chem. Eur. J.* **1997**, *3*, 1151–1159; b) P. M. J. A. Hermans, A. B. Scholten, E. K. van den Beuken, H. C. Brussaard, A. Roelofsen, B. Metz, E. J. Reijerse, P. T. Beurskens, W. P. Bosman, J. M. M. Smits, J. Heck, *Chem. Ber.* **1993**, *126*, 553–563; c) J. Heck, P. M. J. A. Hermans, A. B. Scholten, W. P. J. H. Bosman, G. Meyer, T. Staffel, R. Stürmer, M. Wünsch, *Z. Anorg. Allg. Chem.* **1992**, *611*, 35–42; d) B. Bachmann, F. Hahn, J. Heck, M. Wünsch, *Organometallics* **1989**, *8*, 2523–2542.

[3] U. Behrens, J. Heck, M. Maters, G. Frenzen, A. Roelofsen, H. T. Sommerdijk, *J. Organomet. Chem.* **1994**, *475*, 233–240.

[4] a) J. H. Bieri, T. Egolf, W. von Philipsborn, U. Piantini, R. Prewo, U. Ruppli, A. Salzer, *Organometallics,* **1986**, *5*, 2413–2425; b) W. E.

Table 3. Crystallographic data for **2a**, **3a**, [**3a**]PF_6, and [**3a**]$(BF_4)(PF_6)$.

Compound	**2a**	**3a**	[**3a**]PF_6	[**3a**]$(BF_4)(PF_6)$
formula	$C_{18}H_{19}F_6PRu_2$	$C_{18}H_{18}Ru_2$	$C_{18}H_{18}F_6PRu_2$ ⅓ CH_2Cl_2	$C_{18}H_{18}BF_{10}PRu_2$
mol. mass	582.44	436.46	609.74	668.24
crystal size [mm]	0.37 × 0.29 × 0.21	0.4 × 0.1 × 0.04	0.31 × 0.26 × 0.17	0.31 × 0.26 × 0.17
T [K]	120(2)	173(2)	298(2)	298(2)
space group	*Cmcm*	$P\bar{1}$	*C*2/*c*	*Pnma*
a [pm]	1091.0(3)	766.9(2)	2558.2(11)	1368.16(2)
b [pm]	1403.0(6)	948.5(3)	1717.7(6)	1041.170(10)
c [pm]	1199.3(3)	1163.5(4)	1571.1(8)	1456.94(2)
α [°]	90	68.68(2)	90	90
β [°]	90	74.30(2)	120.19(2)	90
γ [°]	90	66.35(2)	90	90
V [$\times 10^6$ pm^3]	1835.7(10)	714.4(4)	5967(4)	2075.39(5)
Z (no. fomula units)	4	2	12	4
ρ_{calcd} [g cm^{-3}]	2.108	2.029	2.036	2.139
no.collected intensities	3244	4138	14296	11495
no.unique intensities	1460	3274	6887	2693
no.observed intensities[a]	1371	2836	5402	1883
2Θ range [°]	60.0	55.1	56.6	56.86
μ [mm^{-1}]	1.791	2.029	1.744	2.139
min/max transmission	0.478/0.739[b]	[c]	0.66/1.00[d]	0.648/1.000[d]
R_{merg} before/after corr.	0.0699/0.0279	[e]	0.0405/0.0187	0.0482/0.0298
R_{merg} (all data)	0.027	0.021	0.020	0.037
$R1$ (obs. Data)	0.0198	0.0287	0.0468	0.0491
$wR2$ (all data)	0.0488	0.0755	0.1286	0.1549
GOF (F^2, all data)	1.077	1.053	1.005	1.020
residual electron density [e pm^{-9}]	0.41	1.38	2.38	2.48
no. of parameters	77	181	409	179
refinement comments	[f,g]	[h]	[f,g,i]	[f,g,j]
diffractometer[k]	Nicolet R3	Hilger&Watts	Siemens SMART[l]	Siemens SMART[l]

[a] Observation criterion $I > 2\sigma(I)$. [b] Empirical absorption correction based on psi-scans, XEMP (Vers. 4.2) program in SHELXTL package. [c] Not performed. [d] Empirical absorption correction based on equivalent reflections, Siemens-SADABS program. [e] Not determined. [f] SHELXTL (Vers. 5.03) program package used for structure solving with direct methods and refinement on F^2. [g] Hydrogen atoms were located from difference Fourier analyses and were treated as riding groups with free isotropic U values for [**2a**]PF_6, H(6) was refined without constraints; the other hydrogen atoms were positioned at calculated sites and refined as riding groups with the 1.2-fold of the corresponding C atoms. [h] SHELXS 86 program package used for structure solving and SHELXL 93 used for structural refinement. [i] 1.5 Molecules in the asymmetric unit, the CH_2Cl_2 molecule was found disordered. [j] Both, the PF_6 and BF_4 groups are disordered and were refined with constraints to their relative distances. [k] Equiped with graphite monochromized $Mo_{K\alpha}$ radiation. [l] Detector distance 4.457 cm; the standard deviations calculated by the program for the cell dimensions are probably too small and should be multiplied by a factor of 2–10.

Geiger, A. Salzer, J. Edwin, W. von Philipsborn, U. Piantini, A. L. Rheingold, *J. Am. Chem. Soc.* **1990**, *112*, 7113–7121.

[5] L. A. Brady, A. F. Dyke, S. E. Garner, S. A. R. Knox, A. Irving, S. M. Nicholls, A. G. Orpen, *J. Chem. Soc. Dalton Trans.* **1993**, 487–488.

[6] J. Heck, G. Rist, *J. Organomet. Chem.* **1988**, *342*, 45–65.

[7] a) T. P. Gill, K. R. Mann, *Organometallics*, **1982**, *1*, 485–488; b) A. M. McNair, D. C. Boyd, K. R. Mann, *Organometallics*, **1986**, *5*, 303–310.

[8] The hapticity of **1** has been proven by NMR spectroscopy and results from X-ray structure analysis of comparable cyclooctatrienyl compounds (see: J. Heck, G. Lange, O. Reimelt, *Angew. Chem.* **1998**, *110*, 533–535; *Angew. Chem. Int. Ed.* **1998**, *37*, 520–522).

[9] H. Wadepohl, W. Galm, H. Pritzkow, *Organometallics*, **1996**, *15*, 570–576.

[10] The magnetically active Ru isotopes are ^{99}Ru = 12.7 %, and ^{101}Ru = 17.1 %; The nuclear spin is 5/2 for both isotopes, and their gyromagnetic ratio is almost identical.

[11] M. B. Robin, P. Day, *Adv. Inorg. Chem. Radiochem.* **1967**, *10*, 247–422.

[12] C. Creutz, *Prog. Inorg. Chem.* **1983**, *30*, 11–73; N. S. Hush, *Coord. Chem. Rev.* **1985**, *64*, 135–157.

[13] D. E. Richardson, H. Taube, *Coord. Chem. Rev.* **1984**, *60*, 107–129; *Inorg. Chem.* **1981**, *20*, 1278–1285.

[14] For line shape analysis of the dynamic process in **2a** in which the observed nuclei interchange with the rate constant k; the limit of the slow exchange ($k \ll \Delta\omega$) was taken: $k = \pi(\nu_{1/2} - \nu_{o1/2})$ ($\nu_{1/2}$ = half-width of the signal broadened by exchange, $\nu_{o1/2}$ = half-width in the absence of exchange); $\ln k$ as a function of $1/T$ reveals the Arrhenius plot from the slope of which the activation barrier of the molecular fluxionality is calculated to 37 kJ mol^{-1}. The temperature measurements are accurate within ±2 K. (H. Günther, in *NMR-Spektrokopie*, **1992**, 3. Aufl., Thieme, Stuttgart).

[15] J. Edwin, W. E. Geiger, C. Hackett Bushweller, *Organometallics*, **1988**, *7*, 1486–1490; J. Edwin, W. E. Geiger, *J. Am. Chem. Soc.* **1990**, *112*, 7104–7112.

[16] C. Nataro, L. M. Thomas, R. J. Angelici, *Inorg. Chem.* **1997**, *36*, 6000–6008.

[17] A. Salzer, T. Egolf, L. Linowsky, W. Petter, *J. Organomet. Chem.* **1981**, *221*, 339–349.

[18] D. B. Brown, B. F. G. Johnson, C. M. Martin, S. Parsons, *J. Organomet. Chem.* **1997**, 285–291.

[19] B. Bachmann, G. Baum, J. Heck, W. Massa, B. Ziegler, *Z. Naturforsch. B* **1990**, *45*, 221–238.

[20] A. J. P. Domingos, B. F. G. Johnson, J. Lewis, G. M. Sheldrick, *J. Chem. Soc. Commun.* **1973**, 912–913; G. Gervasio, D. Osella, M. Valle, *Inorg. Chem.* **1976**, *15*, 1221–1224; M. R. Churchill, B. G. De Boer, F. J. Rotella, *Inorg. Chem.* **1976**, *15*, 1843–1853; M. Catti, G. Gervasio, S. A. Mason, *J. Chem. Soc. Dalton Trans.* **1977**, 2260–2264; T. V. Ashworth, D. C. Liles, E. Singleton, *J. Chem. Soc. Chem. Comm.* **1984**, 1317–1318.

[21] R. G. Teller, R. Bau, *Strukt. Bonding (Berlin)* **1981**, *44*, 1–82.

[22] D. M. Antonelli, M. Cowie, *Organometallics* **1990**, *9*, 1818–1826; M. D. Antonelli, M. Cowie, *Inorg. Chem.* **1990**, *29*, 4039–4045; G. de Leeuw, J. S. Field, R. J. Haines, *J. Organomet. Chem.* **1989**, *359*, 245–254; J. S. Field, R. J. Haines, L. A. Rix, *J. Chem. Soc. Dalton Trans.* **1990**, 2311–2314; J. L. Petersen, R. P. Stewart, *Inorg. Chem.*

1980, *19*, 186–191; D. J. Elliot, J. J. Vittal, R. J. Puddephatt, D. G. Holah, A. N. Hughes, *Inorg. Chem.* **1992**, *31*, 1247–1250.
[23] U. T. Müller-Westerhoff, A. Rheingold, G. Swiegers, *Angew. Chem.* **1992**, *104*, 1398–1400; *Angew. Chem. Int. Ed. Engl.* **1992**, *31*, 1352–1354.
[24] Results of theoretical work are in agreement with the MO model of the metal–metal bonding in μ-(η^5:η^5-cot) complexes; U. Richter, J. Heck, J. Reinhold, *Inorg. Chem.*, in press.
[25] D. J. Brauer, C. Krüger, *Inorg. Chem.* **1976**, *15*, 2511–2514.
[26] J. W. Lauher, R. Hoffmann, *J. Am. Chem. Soc.* **1976**, *98*, 1729–1742.
[27] M. R. Churchill, F. Rotella, B. King, M. N. Ackermann, *J. Organomet. Chem.* **1975**, C15–C18.
[28] E. B. Fleischer, A. L. Stone, R. B. K. Dewar, J. D. Wright, C. E. Keller, R. Pettit, *J. Am. Chem. Soc.* **1966**, *88*, 3159–3161.

Received: June 15, 1998
Revised version: September 15 1998 [F 1206]

0947-6539/99/0502-0668 $ 17.50+.50/0